

Monitoring statistics of the ERS-2 scatterometer for ESA

Cycle 150

(Project Ref. 22025/08/I-EC)

Hans Hersbach
European Centre for Medium-Range Weather Forecasts,
Shinfield Park, Reading, RG2 9AX, England
Tel: (+44 118) 9499476, e-mail: dal@ecmwf.int

October 1, 2009

1 Introduction

The quality of the UWI product was monitored at ECMWF for Cycle 150. Results were compared to those obtained from the previous Cycle, as well for data received during the nominal period in 2000 (up to Cycle 59). No corrections for duplicate observations from overlapping ground stations were applied.

During Cycle 150 data was received between 21:05 UTC 24 August 2009 and 21:00 UTC 28 September 2009. Data was grouped into 6-hourly batches (centred around 00, 06, 12 and 18 UTC). No data was received for the batch for 18 UTC 4 September 2009, and for batches between 18 UTC 9 September and 12 UTC 10 September 2009.

Data is being recorded whenever within the visibility range of a ground station. No data from Johannesburg was received. For Cycle 150, data coverage was over the North-Atlantic, part of the Mediterranean, the Gulf of Mexico, a very small part of the Pacific west from the US, Canada and Central America, the Chinese Sea, a small part of the Indian Ocean south-east from Thailand and Indonesia, and an area South from Australia (see Figure 2).

Time series of the asymmetry between the fore and aft incidence angles show a calm behaviour.

Compared to Cycle 149, the UWI wind speed relative to ECMWF first-guess (FG) fields showed a higher standard deviation (1.38 m/s, was 1.32 m/s). Bias levels were less negative (on average -1.01 m/s, was -1.12 m/s).

Ocean calibration shows that inter-node and inter-beam dependencies of bias levels were reduced compared to those for Cycle 149. Average bias levels were less negative

(-0.72 dB, was -0.95 dB; see Figure 4).

The ECMWF operational assimilation was changed on 8 September 2009. A non-orographic gravity wave scheme was introduced, and the wave damping in wind input source term for ocean waves was improved. Regarding assimilation, cloud-affected radiances for infra-red instruments, total column water vapour data from MERIS over land, and ASCAT data from the EARS service were introduced. The impact on the quality of surface wind is expected to be minor.

The Cycle-averaged evolution of performance relative to ECMWF first-guess (FG) winds is displayed in Figure 1. Figure 2 shows global maps of the over Cycle 150 averaged UWI data coverage and wind climate, Figure 3 for performance relative to FG winds.

2 ERS-2 statistics from 24 August 2009 to 28 September 2009

2.1 Sigma0 bias levels

The average sigma0 bias levels (compared to simulated sigma0's based on ECMWF model FG winds) stratified with respect to antenna beam, ascending or descending track and as function of incidence angle (i.e. across-node number) is displayed in Figure 4.

Compared to Cycle 149, inter-node and inter-beam dependencies between the fore and aft antenna have improved. A rather big asymmetry between the mid and fore/aft antenna for ascending tracks was diminished. Average bias level was less negative (-0.72 dB, was -0.95 dB), being 0.3 dB more negative than nominal data in 2000 (around -0.4 dB; see Figure 1 of the reports for Cycle 48 to 59). The situation is slightly better to that of one year ago (see report for Cycle 140).

Long-term variations correlate with the yearly cycle, which, given the non-global coverage, is understandable. Therefore, the method of ocean calibration will probably only provide accurate information on calibration levels for globally or yearly averaged data sets.

The data volume of descending tracks was about 23% lower than for ascending tracks.

2.2 Incidence angles

For ESACA, across-node binning is, like the old processor, retained on a 25km mesh. From simple geometrical arguments it follows that variations in yaw attitude will lead to asymmetries between the incidence angles of the fore and aft beam. Indeed, this has been observed. Figure 5 gives a time evolution of this asymmetry. Also in this Figure, the occasions for which the combined k_p -yaw quality flag was set are indicated by red stars. The relation with incidence-angle asymmetries is obvious.

The asymmetry between the fore and aft incidence angles was relatively calm. There were virtually no solar spots, although some magnetic storms did hit the Earth around 2 September and 28 September 2009 (source www.spaceweather.com).

2.3 Distance to cone history

The distance to the cone history is shown in Figure 6. Curves are based on data that passed all QC, including the test on the k_p -yaw flag, and subject to the land and sea-ice check at ECMWF (see cyclic report 88 for details).

Like for previous Cycles, time series are (due to lack of statistics) very noisy, especially for the near-range nodes. Most spikes were found to be the result of low data volumes.

Compared to Cycle 149, the average level was reduced considerably (1.16 was 1.24), and is higher (by 6%) than for nominal data (see top panel Figure 1).

The fraction of data that did not pass QC is displayed in Figure 6 as well (dashed curves).

2.4 UWI minus First-Guess wind history

In Figure 7, the UWI minus ECMWF first-guess wind-speed history is plotted. The history plot shows a few peaks, which are usually the result of low data volume.

Figure 11 displays the locations for which UWI winds were more than 8 m/s weaker (top panel), respectively more than 8 m/s stronger (lower panel) than FG winds. Like for Cycle 149, such collocations are isolated, and often indicate meteorologically active regions, for which UWI data and ECMWF model field show reasonably small differences in phase and/or intensity. Deviations near the poles are the result of imperfect sea-ice flagging.

Two cases for which UWI winds were considerably different from FG winds are presented in Figure 12. A case in the North Atlantic on 18 September 2009 (top panel) shows a patch of UWI winds with de-aliasing problems, and some winds with noisy direction at low incidence angle (left-hand track), as well. A case in the Tasman Sea for 29 August 2009 (lower panel) displays a small relative shift in a weather front.

Average bias levels and standard deviations of UWI winds relative to FG winds are displayed in Table 1. From this it follows that the bias of UWI winds was less negative (-1.01 m/s, was -1.12 m/s), being around 0.2 m/s more biased low than nominal data in 2000.

On a longer time scale seasonal bias trends are observed (see Figure 1). The large increase in negative bias that had emerged a few Cycles ago, and its current reduction are typical for this season. As was highlighted in previous cyclic reports, it is believed that this yearly trend is partly induced by changing local geophysical conditions. Indication for this is a similar trend observed for QuikSCAT data when restricted to an area well-covered by ERS-2 (20N-90N, 80W-20E). Figure 17 shows time series for that area for both ERS-2 (top panel) and QuikSCAT (lower panel) for the period between 1 January 2004 and 28 September 2009 (end of Cycle 150). Results are displayed for at ECMWF actively assimilated data, i.e., CMOD5/CMOD5.4 winds for ERS-2 and 4%-reduced QuikSCAT winds on a 50km resolution. Note the increase in ERS-2 wind speed as used at ECMWF since the introduction of the new ECMWF model cycle on 7 June 2007 (Figure 17). It reflects a switch at ECMWF from the CMOD5 to CMOD5.4 model function, which has enhanced the scatterometer wind (as used at ECMWF) by 0.48 m/s.

	Cycle 149		Cycle 150	
	UWI	CMOD4	UWI	CMOD4
speed STDV	1.32	1.32	1.38	1.37
node 1-2	1.40	1.38	1.43	1.42
node 3-4	1.33	1.32	1.36	1.35
node 5-7	1.28	1.28	1.32	1.32
node 8-10	1.26	1.26	1.35	1.35
node 11-14	1.27	1.28	1.34	1.34
node 15-19	1.30	1.30	1.35	1.35
speed BIAS	-1.12	-1.12	-1.01	-1.02
node 1-2	-1.61	-1.59	-1.53	-1.51
node 3-4	-1.39	-1.35	-1.29	-1.25
node 5-7	-1.16	-1.14	-1.06	-1.03
node 8-10	-0.98	-0.98	-0.87	-0.87
node 11-14	-0.92	-0.95	-0.82	-0.83
node 15-19	-0.93	-0.97	-0.82	-0.86
direction STDV	30.1	18.6	29.0	18.5
direction BIAS	-1.7	-2.0	-1.9	-2.3

Table 1: Biases and standard deviation of ERS-2 versus ECMWF FG winds in m/s for speed and degrees for direction.

The standard deviation of UWI wind speed versus ECMWF FG has, compared to Cycle 149, increased (1.38 m/s, was 1.32 m/s).

For Cycle 150 the (UWI - FG) direction standard deviations were mostly ranging between 20 and 40 degrees (Figure 8). Average STDV for UWI wind direction was reduced compared to that of Cycle 149 (29.0 degrees, was 30.1 degrees). For at ECMWF de-aliased winds (Figure 10) performance basically appeared unchanged (STDV 18.5, was 18.6 degrees).

2.5 Scatterplots

Scatterplots of FG winds versus ERS-2 winds are displayed in Figures 13 to 16. Values of standard deviations and biases are slightly different from those displayed in Table 1. Reason for this is that, for plotting purposes, the in 0.5 m/s resolution ERS-2 winds have been slightly perturbed (increases scatter with 0.02 m/s), and that zero wind-speed ERS-2 winds have been excluded (decreases scatter by about 0.05 m/s).

The scatterplot of UWI wind speed versus FG (Figure 13) is very similar to that for (at ECMWF inverted) de-aliased CMOD4 winds (Figure 15). It confirms that the ESACA inversion scheme is working properly.

Winds derived on the basis of CMOD5 are displayed in Figure 16. The relative standard deviation is lower than for CMOD4 winds (1.35 m/s versus 1.40 m/s). Compared to ECMWF FG, CMOD5 winds are 0.53 m/s slower.

Figure Captions

Figure 1: Evolution of the performance of the ERS-2 scatterometer averaged over 5-weekly Cycles from 12 December 2001 (Cycle 69) to 28 September 2009 (end Cycle 150) for the UWI product (solid, star) and de-aliased winds based on CMOD4 (dashed, diamond). Results are based on data that passed the UWI QC flags. For Cycle 85 two values are plotted; the first value for a global set, the second one for a regional set (for details see the corresponding cyclic report). Dotted lines represent values for Cycle 59 (5 December 2000 to 17 January 2001), i.e. the last stable Cycle of the nominal period. From top to bottom panel are shown the normalized distance to the cone (CMOD4 only) the standard deviation of the wind speed compared to FG winds, the corresponding bias (for UWI winds the extremes in node-wise averages are shown as well), and the standard deviation of wind direction compared to FG.

Figure 2: Average number of observations per 12H and per 125km grid box (top panel) and wind climate (lower panel) for UWI winds that passed the UWI flags QC and a check on the collocated ECMWF land and sea-ice mask.

Figure 3: The same as Figure 2, but now for the relative bias (top panel) and standard deviation (lower panel) with ECMWF first-guess winds.

Figure 4: Ratio of $\langle \sigma_0^{0.625} \rangle / \langle \text{CMOD4}(\text{FirstGuess})^{0.625} \rangle$ converted in dB for the fore beam (solid line), mid beam (dashed line) and aft beam (dotted line), as a function of incidence angle for descending and ascending tracks. The thin lines indicate the error bars on the estimated mean. First-guess winds are based on the in time closest (+3h, +6h, +9h, or +12h) T799 forecast field, and are bilinearly interpolated in space.

Figure 5: Time series of the difference in incidence angle between the fore and aft beam. Red stars indicate the occurrences for which the combined k_p -yaw flag was set.

Figure 6: Mean normalized distance to the cone computed every 6 hours for nodes 1-2, 3-4, 5-7, 8-10, 11-14 and 15-19). The dotted curve shows the number of incoming triplets in logarithmic scale (1 corresponds to 60,000 triplets) and the dashed one indicates the fraction of complete (based on the land and sea-ice mask at ECMWF) sea-located triplets rejected by ESA flags, or by the wind inversion algorithm (0: all data kept, 1: no data kept).

Figure 7: Mean (solid line) and standard deviation (dashed line) of the wind speed difference UWI - first guess for the data retained by the quality control.

Figure 8: Same as Fig. 7, but for the wind direction difference. Statistics are computed for winds stronger than 4 m/s.

Figures 9 and 10: Same as Fig. 7 and 8 respectively, but for the de-aliased CMOD4 data.

Figure 11: Locations of data during Cycle 150 for which UWI winds are more than 8 m/s weaker (top panel) respectively stronger (lower panel) than FG, and on which QC on UWI flags and the ECMWF land/sea-ice mask was applied.

Figure 12: Comparison of UWI winds (in red) with ECMWF FG winds (in blue) for a case on 18 September 2009 (top panel) in the Atlantic and a case on 29 August 2009 (lower panel) in the Tasman Sea.

Figure 13: Two-dimensional histogram of first guess and UWI wind speeds, for the data kept by the UWI flags, and QC based on the ECMWF land and sea-ice mask. Circles

denote the mean values in the y-direction, and squares those in the x-direction.

Figure 14: Same as Fig. 13, but for wind direction. Only winds stronger than 4m/s are taken into account.

Figure 15: Same as Fig. 13, but for de-aliased CMOD4 winds.

Figure 16: Same as Fig. 13, but for de-aliased CMOD5 winds.

Figure 17: Wind-speed bias relative to FG winds for actively assimilated ERS-2 winds (based on CMOD5 before 7 June 2007; CMOD5.4 afterwards) for nodes 1-19 (top panel) respectively 50-km QuikSCAT (based on the QSCAT-1 model function and reduced by 4%) for nodes 5-34 (lower panel), averaged over the area (20N-90N, 80W-20E), and displayed for the period 1 January 2004 - 28 September 2009. Fat curves represent centred 15-day running means, thin curves values for 6-hourly periods. Vertical dashed blue lines mark ECMWF model changes.

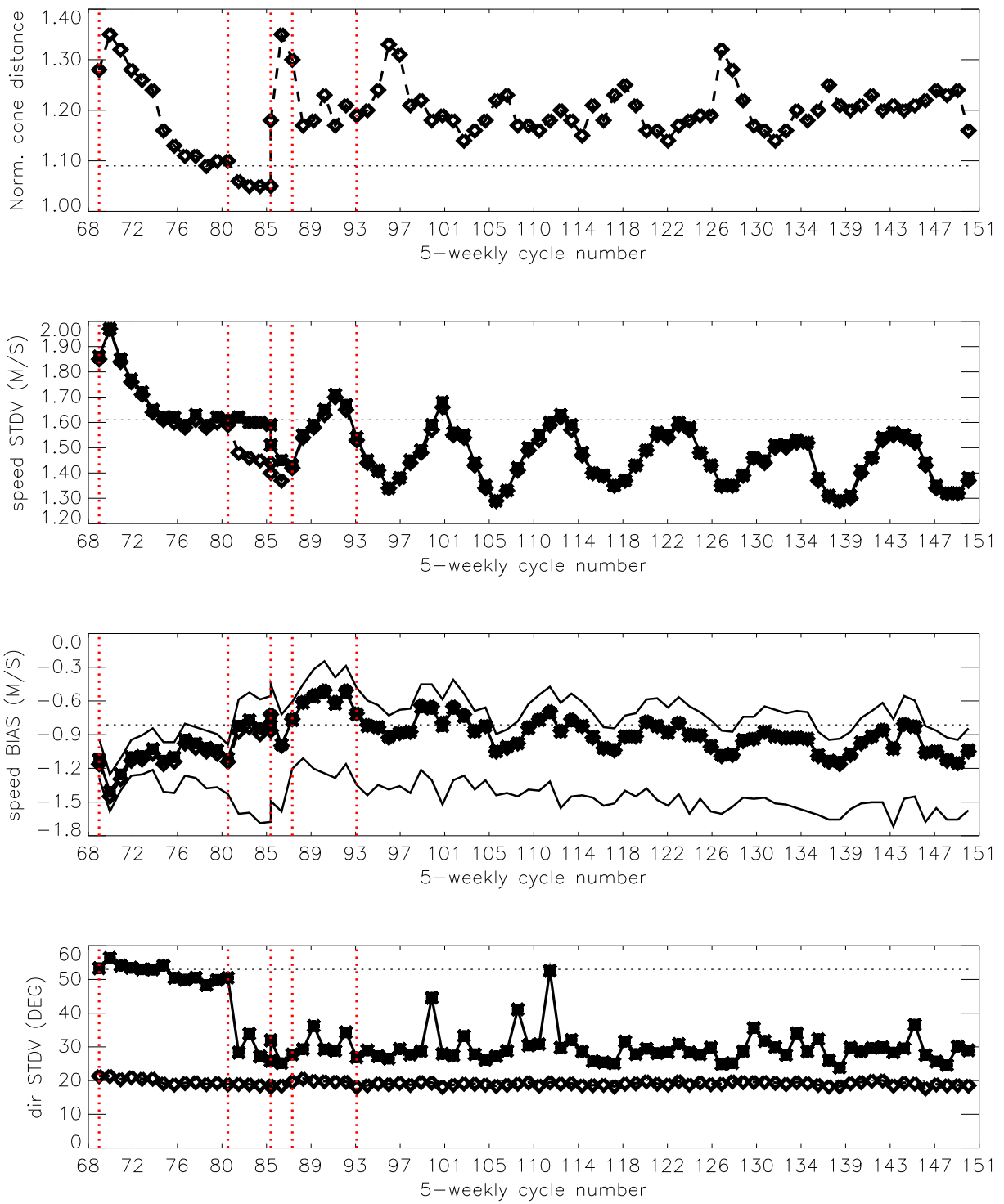
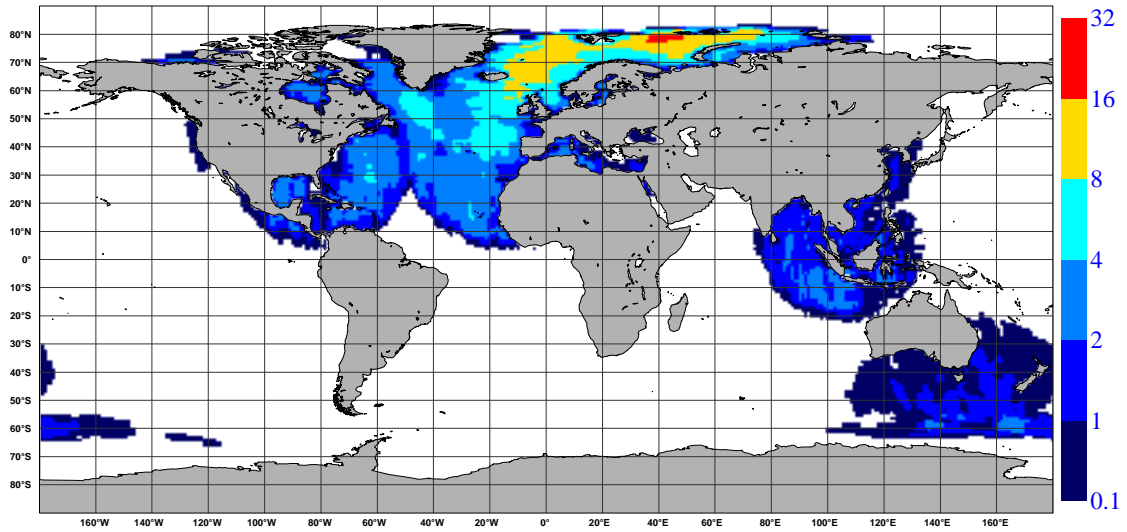


Figure 1

NOBS (ERS-2 UWI), per 12H, per 125km box
average from 2009082500 to 2009092818 GLOB:1.89



AVERAGE (ERS-2 UWI), in m/s.
average from 2009082500 to 2009092818 GLOB:6.48

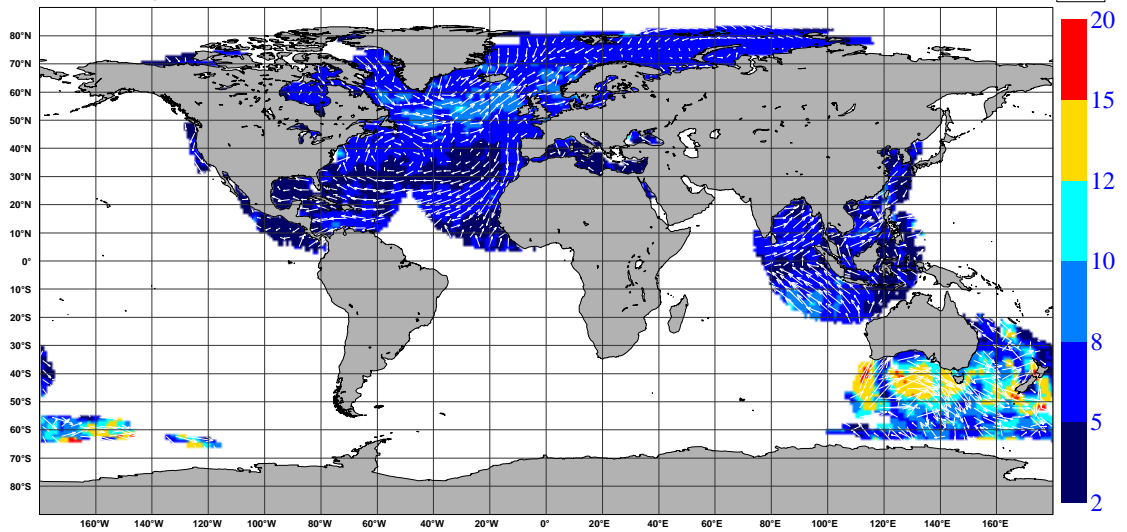
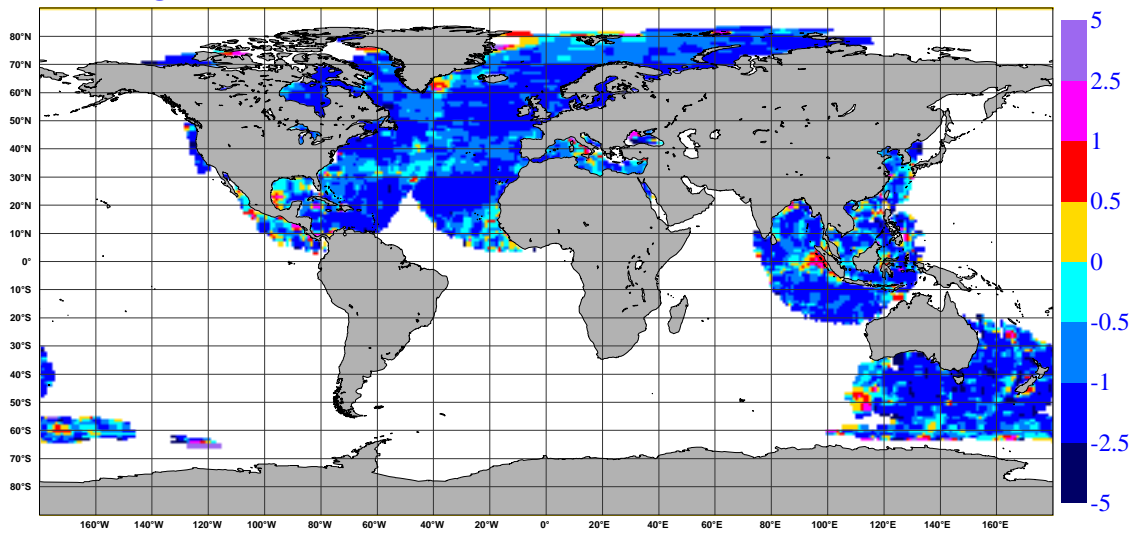


Figure 2

BIAS (ERS-2 UWI vs FIRST-GUESS), in m/s.
average from 2009082500 to 2009092818 GLOB:-1



STDV (ERS-2 UWI vs FIRST-GUESS), in m/s.
average from 2009082500 to 2009092818 GLOB:1.12

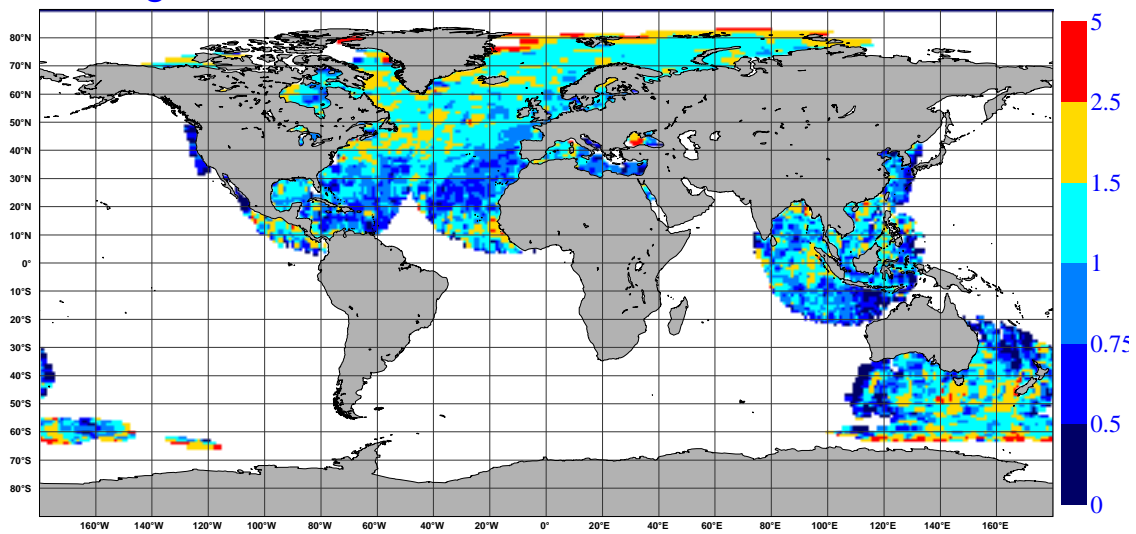
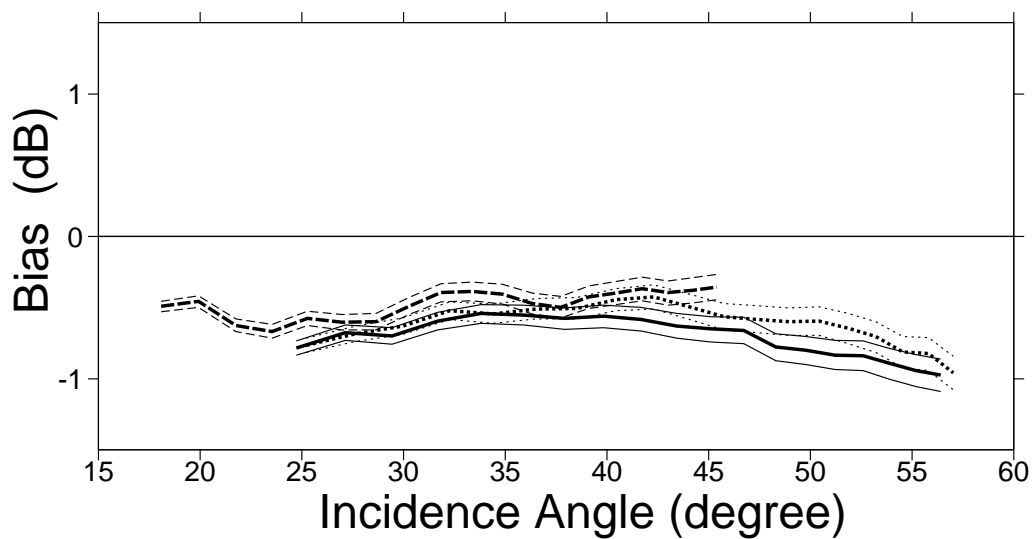


Figure 3

BIAS: $(s_{0obs}^{**0.625}) / (s_{0fg3h}^{**0.625})$
ERS-2 obs. from 24/08/2009 21:05 UTC to 28/09/2009 21:00 UTC
DESCENDING TRACKS
385372 Entries, 46.3 % used (flat wind dir. dist.)
___ Fore __Mid ...Aft thin: Error Bar



BIAS: $(s_{0obs}^{**0.625}) / (s_{0fg3h}^{**0.625})$
ERS-2 obs. from 24/08/2009 21:05 UTC to 28/09/2009 21:00 UTC
ASCENDING TRACKS
503149 Entries, 56.6 % used (flat wind dir. dist.)
___ Fore __Mid ...Aft thin: Error Bar

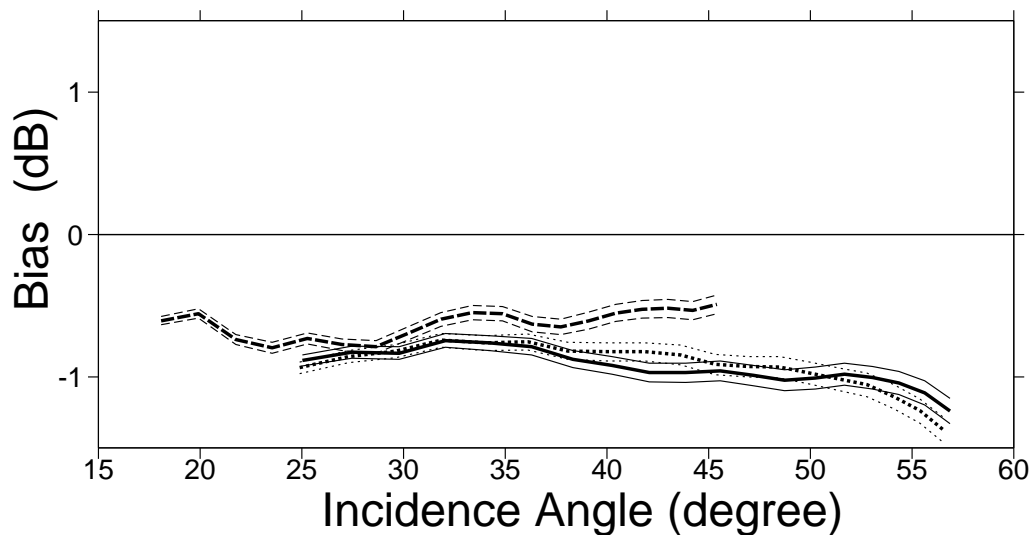


Figure 4

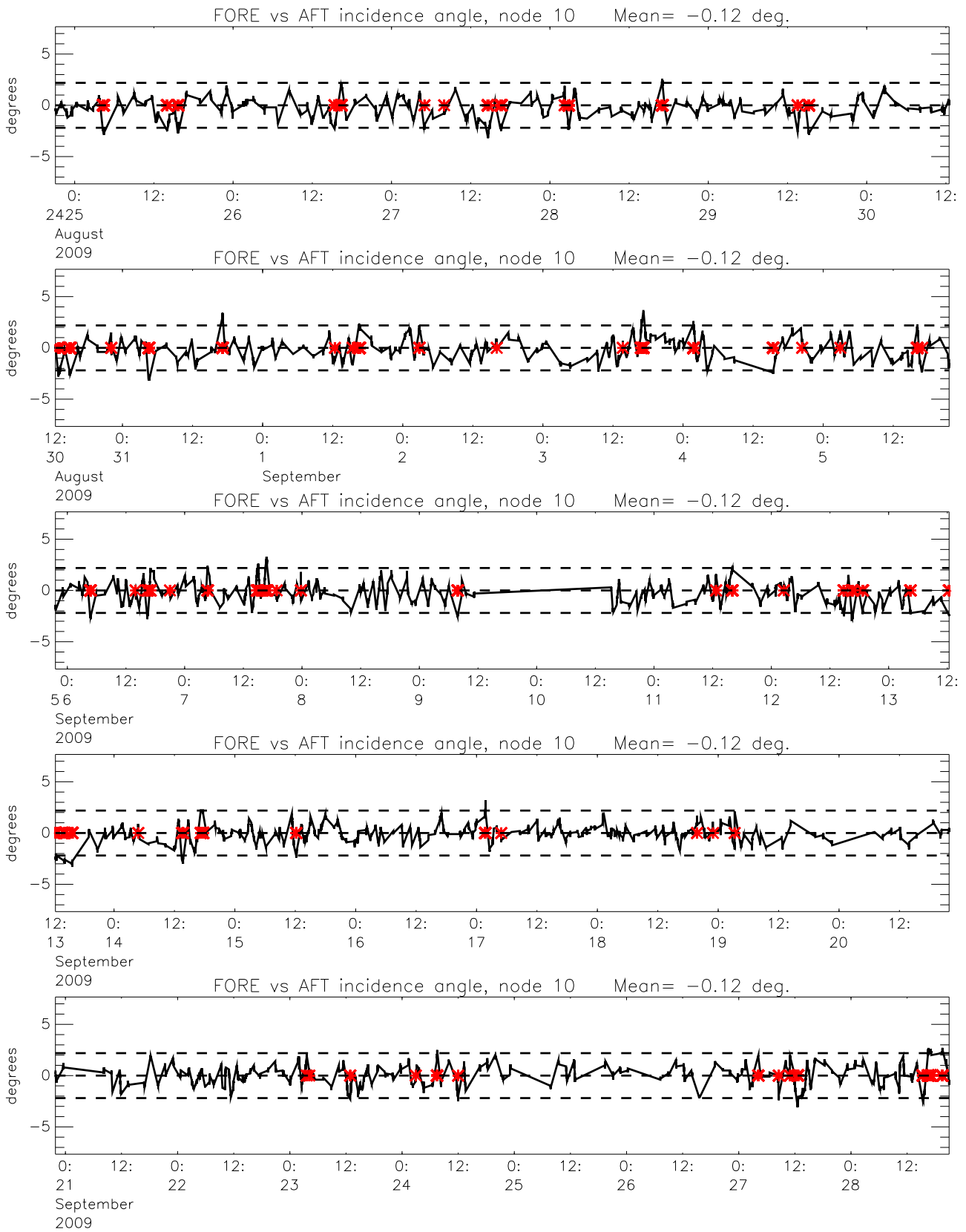


Figure 5

Monitoring of Sigma0 triplets versus CMOD4 for ERS-2

from 2009082500 to 2009092818

(solid) mean normalised distance to the cone over 6 h

(dashed) fraction of complete sea-point observations rejected by ESA flag or CMOD4 inversion

(dotted) total number of data in log. scale (1 for 60000)

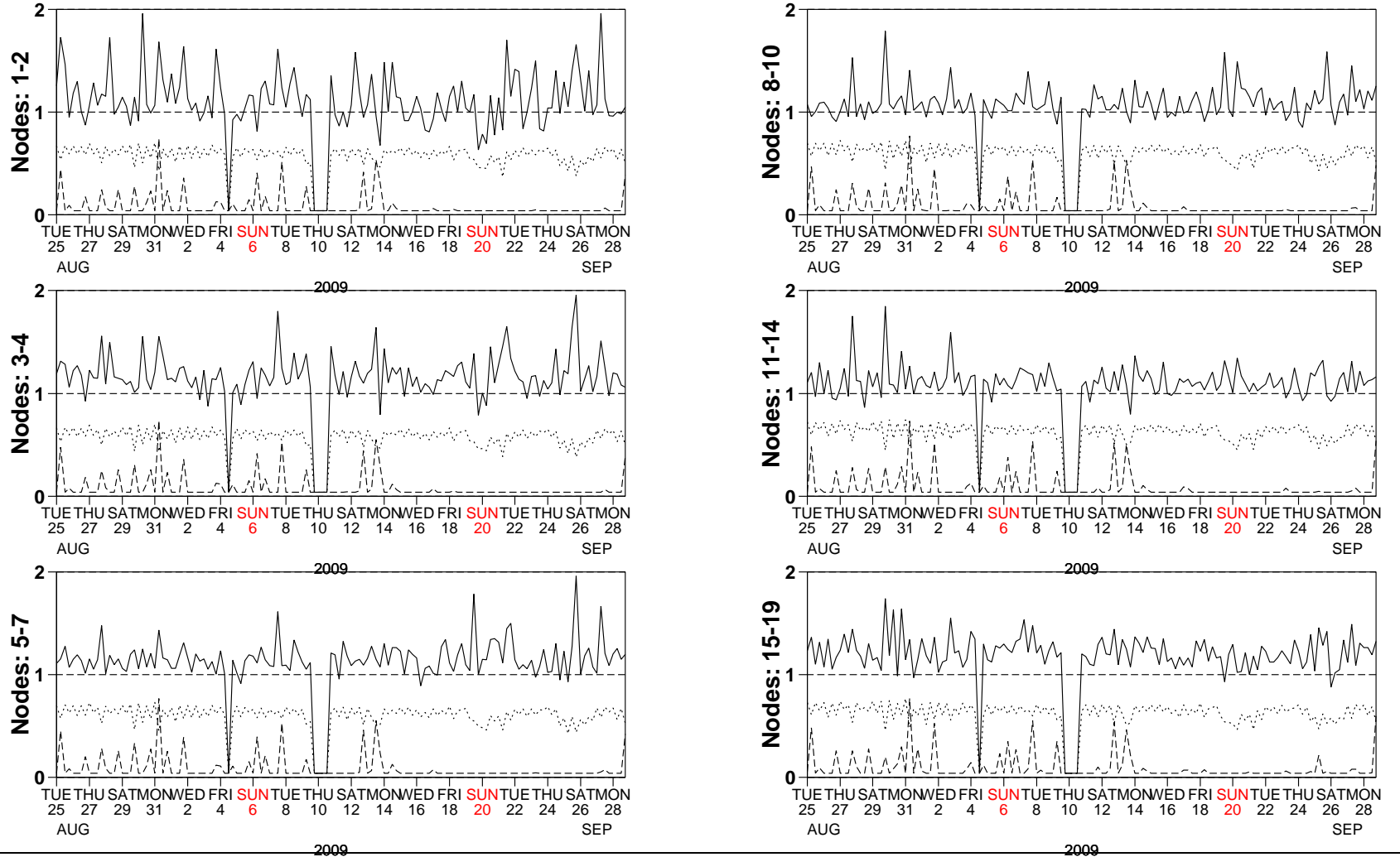


Figure 6

Monitoring of UWI winds versus First Guess for ERS-2

from 2009082500 to 2009092818

(solid) wind speed bias UWI - First Guess over 6h (deg.)

(dashed) wind speed standard deviation UWI - First Guess over 6h (deg.)

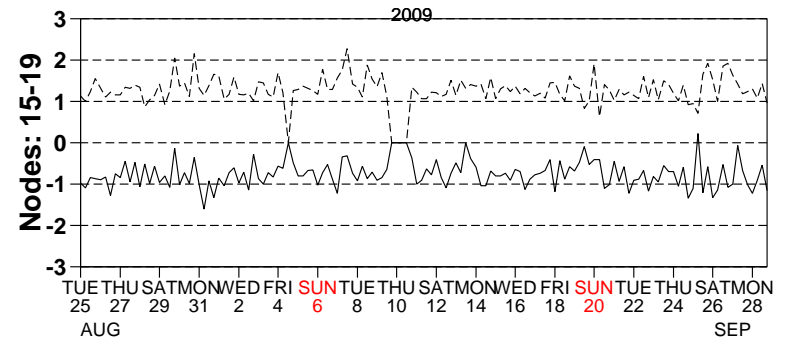
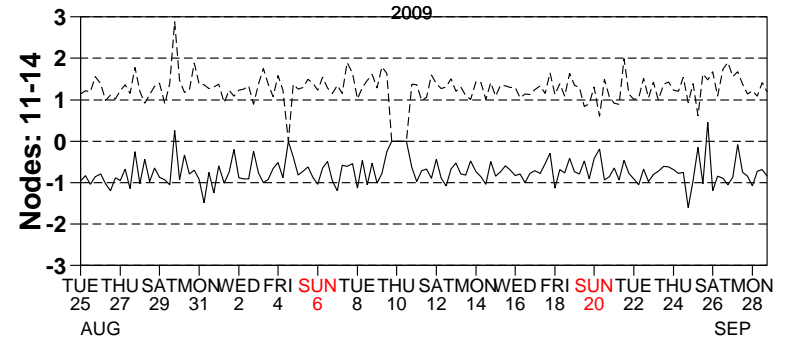
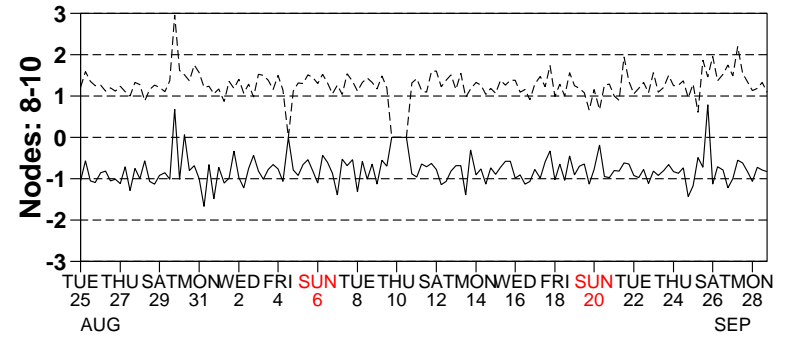
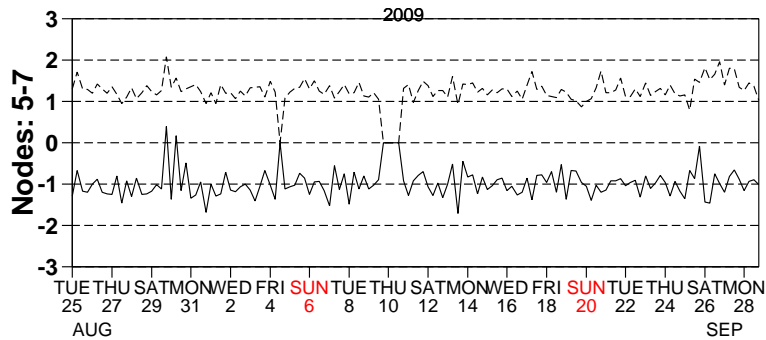
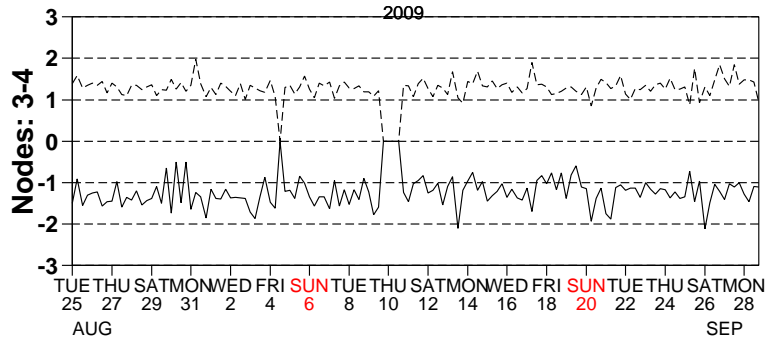
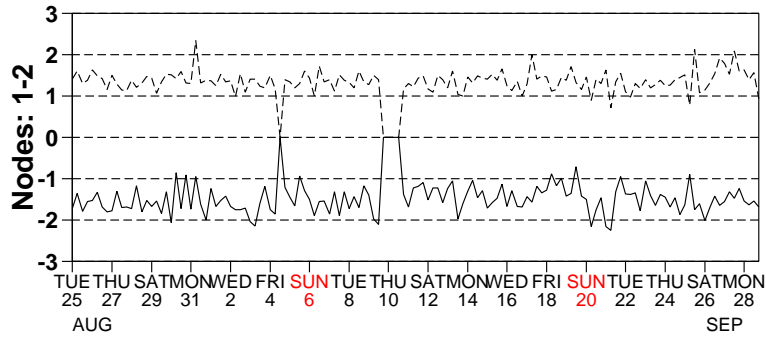


Figure 7

Monitoring of UWI winds versus First Guess for ERS-2

from 2009082500 to 2009092818

(solid) wind direction bias UWI - First Guess over 6h (deg.)

(dashed) wind direction standard deviation UWI - First Guess over 6h (deg.)

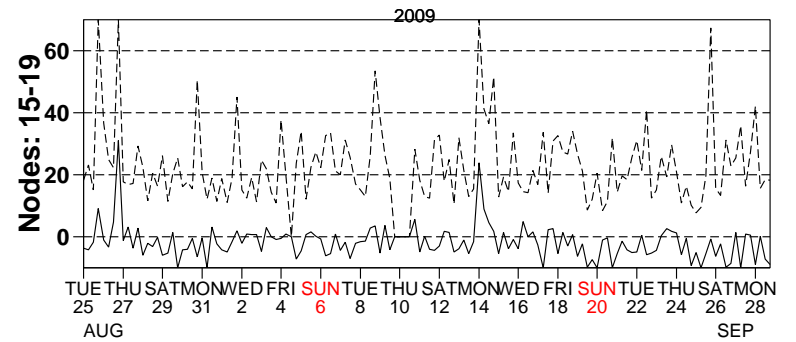
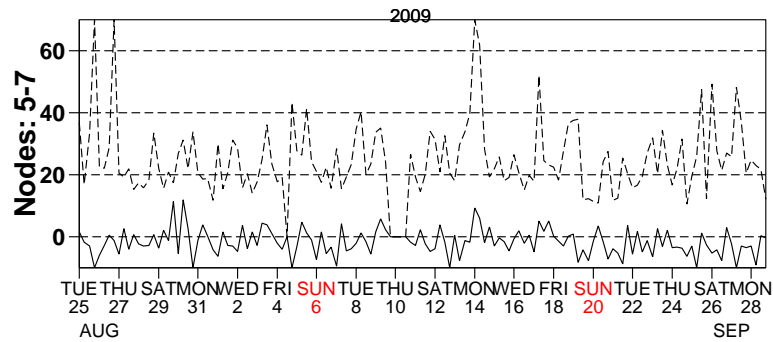
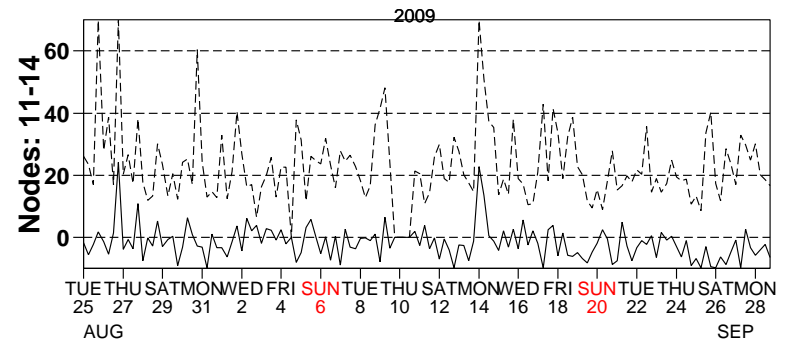
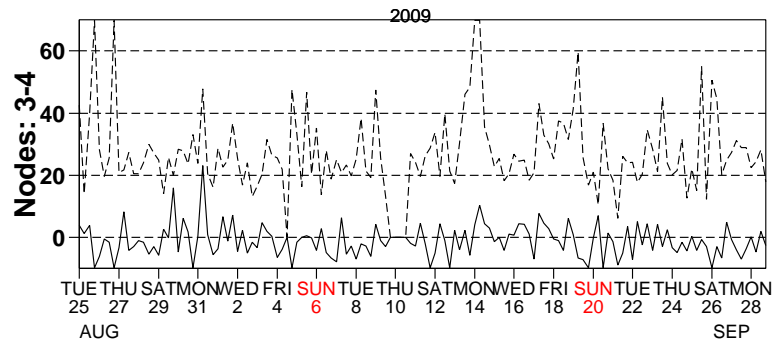
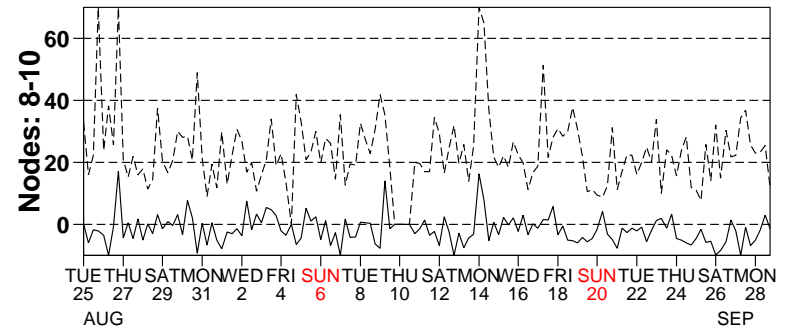
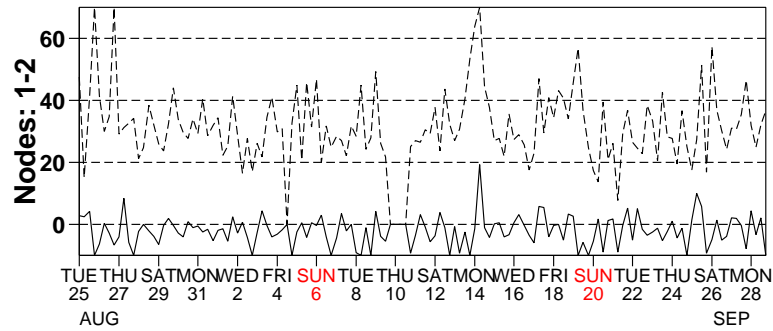


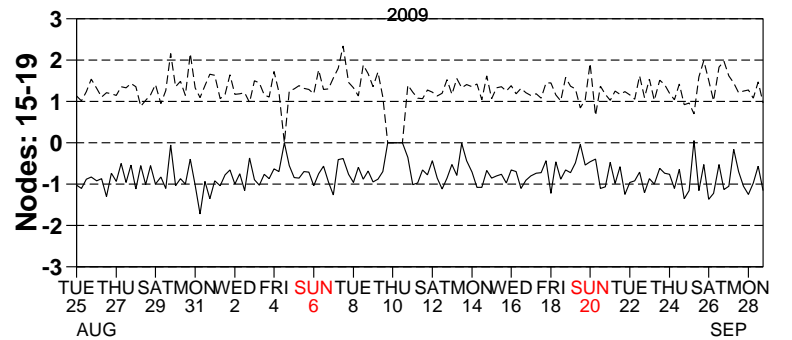
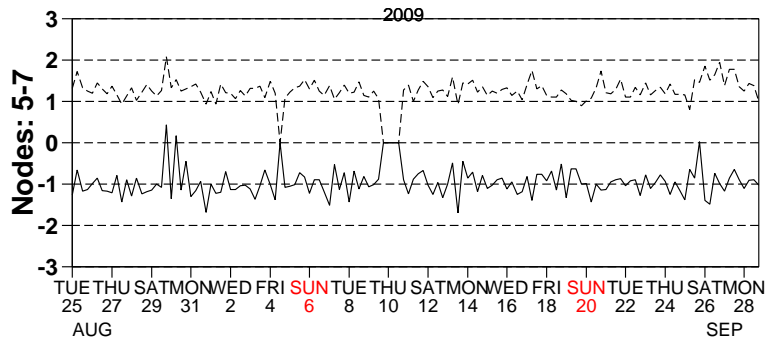
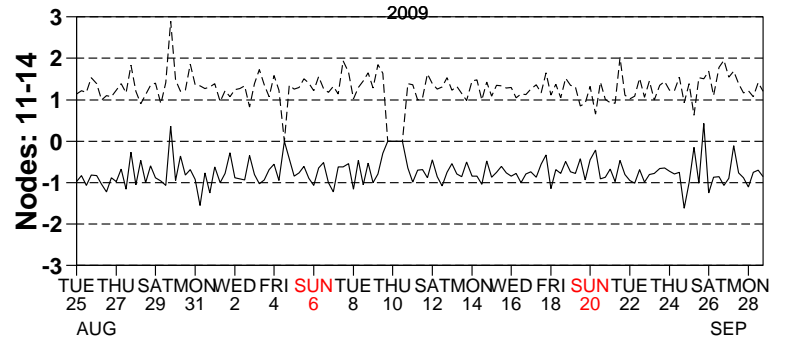
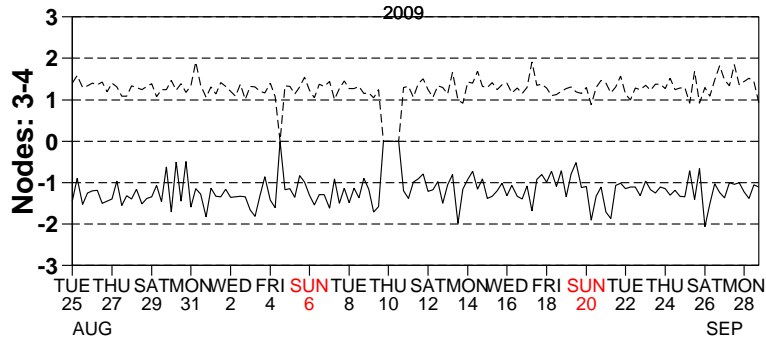
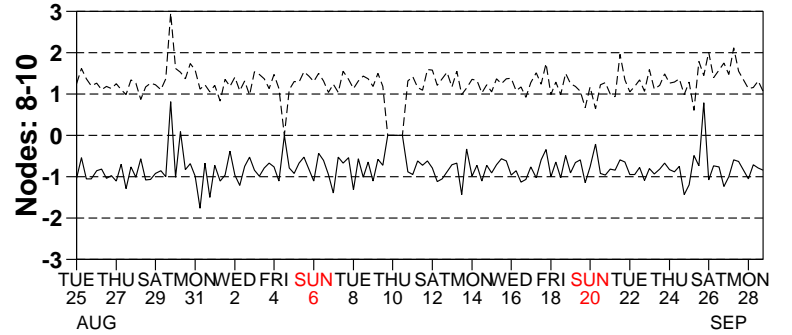
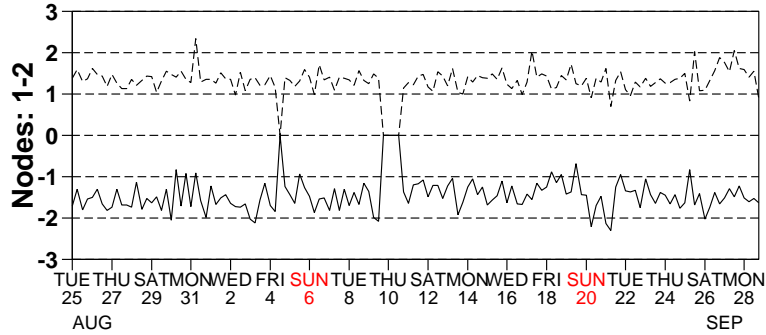
Figure 8

Monitoring of de-aliased CMOD4 winds versus First Guess for ERS-2

from 2009082500 to 2009092818

(solid) wind speed bias CMOD4 - First Guess over 6h (deg.)

(dashed) wind speed standard deviation CMOD4 - First Guess over 6h (deg.)



2009

2009

Figure 9

Monitoring of de-aliased CMOD4 winds versus First Guess for ERS-2

from 2009082500 to 2009092818

(solid) wind direction bias CMOD4 - First Guess over 6h (deg.)

(dashed) wind direction standard deviation CMOD4 - First Guess over 6h (deg.)

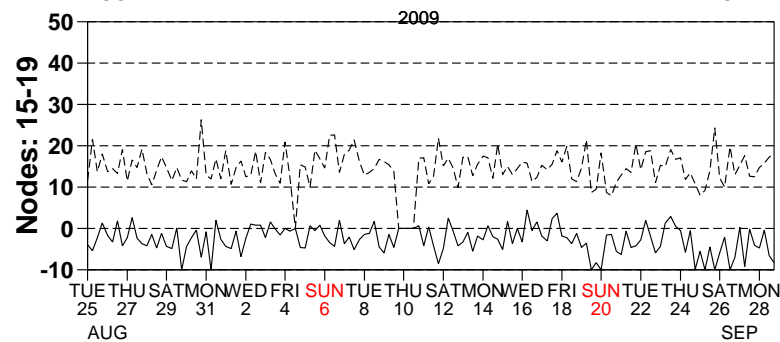
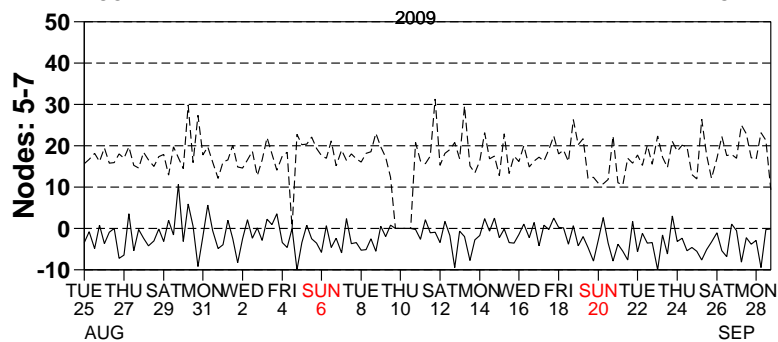
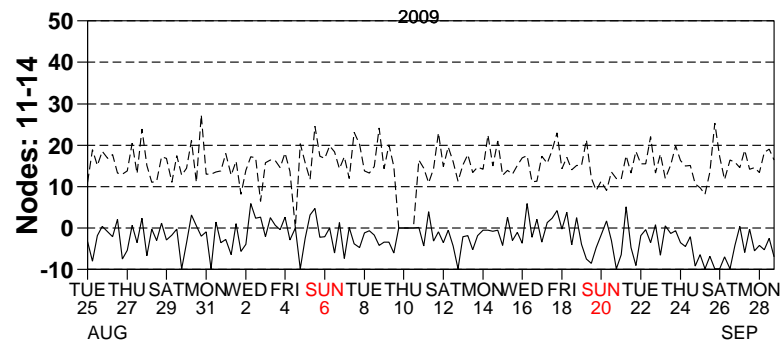
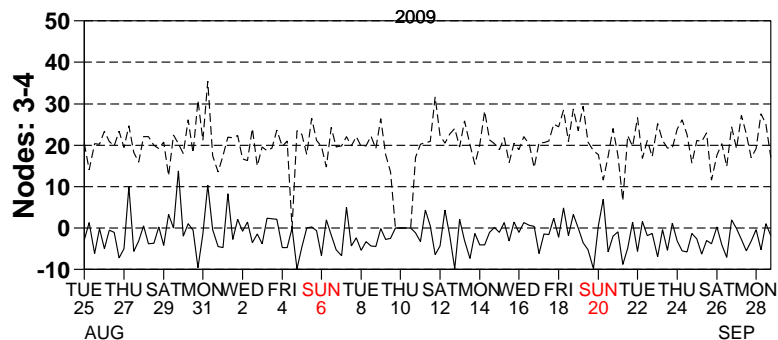
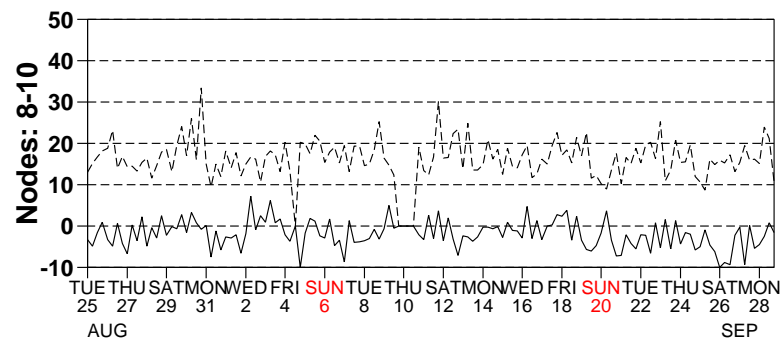
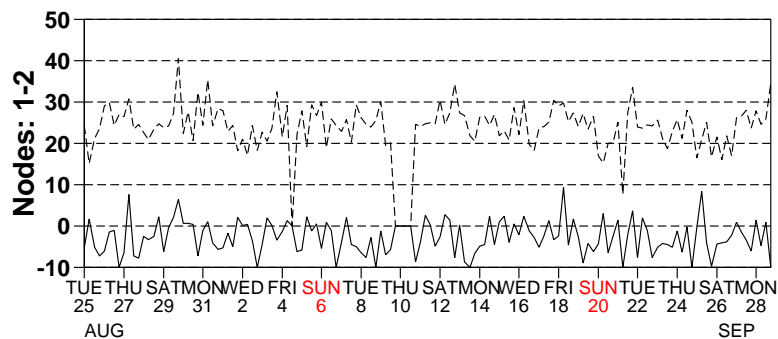
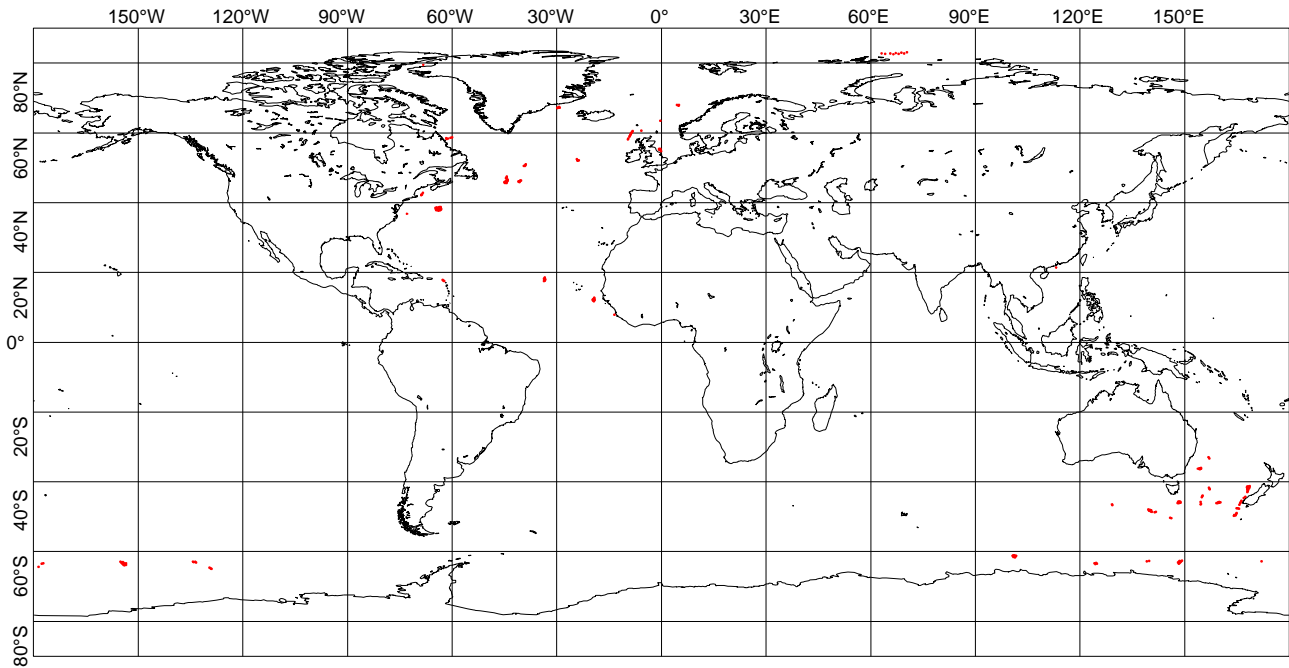


Figure 10

UWI winds more than 8 m/s weaker than ECMWF First Guess
CYCLE 150, 2009082500 to 2009092818, QC on ESA flags



UWI winds more than 8 m/s stronger than ECMWF First Guess
CYCLE 150, 2009082500 to 2009092818, QC on ESA flags

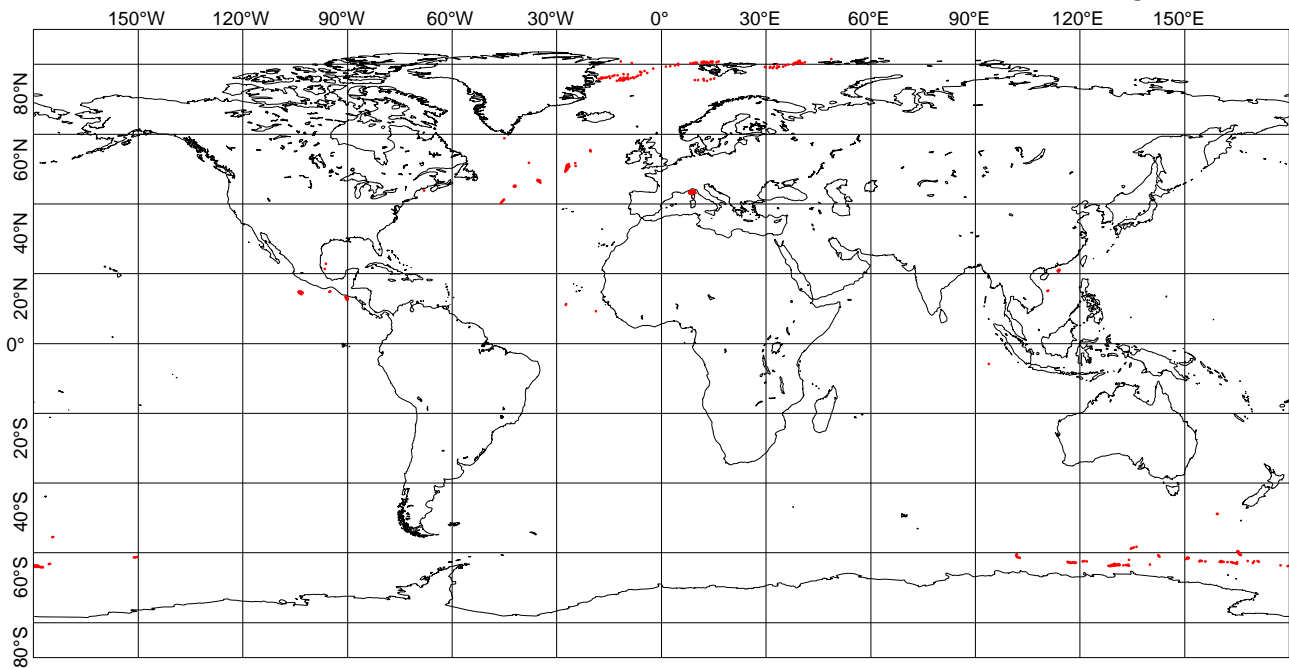
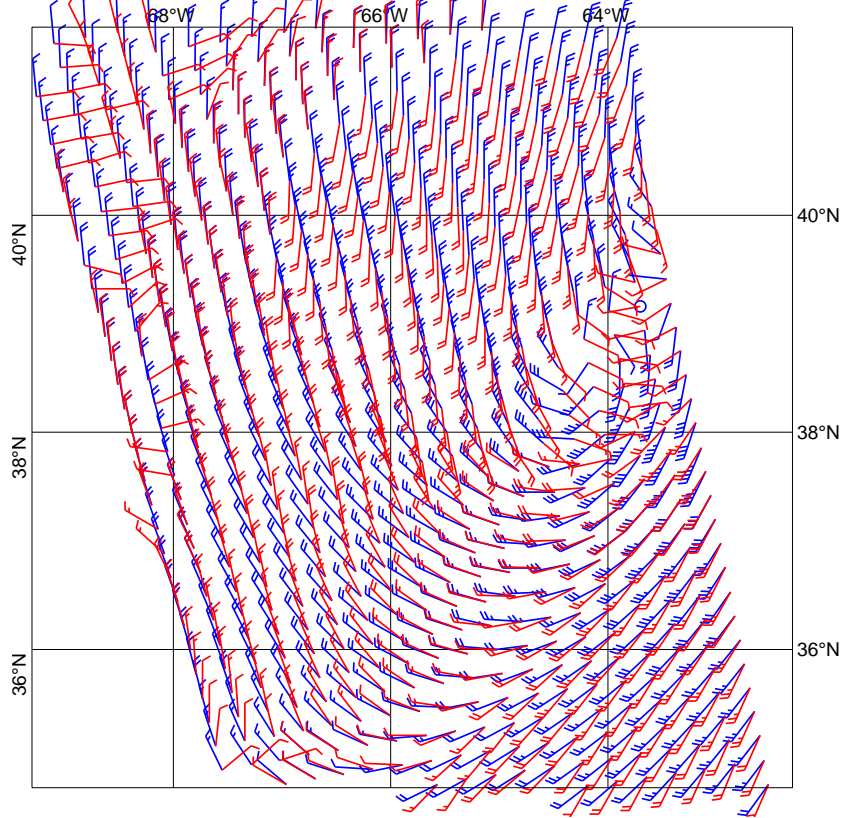


Figure 11

UWI winds (red) versus ECMWF FG winds (blue)
North Atlantic 20090918 02:48 UTC



UWI winds (red) versus ECMWF FG winds (blue)
Tasman Sea 20090829 22:35 UTC

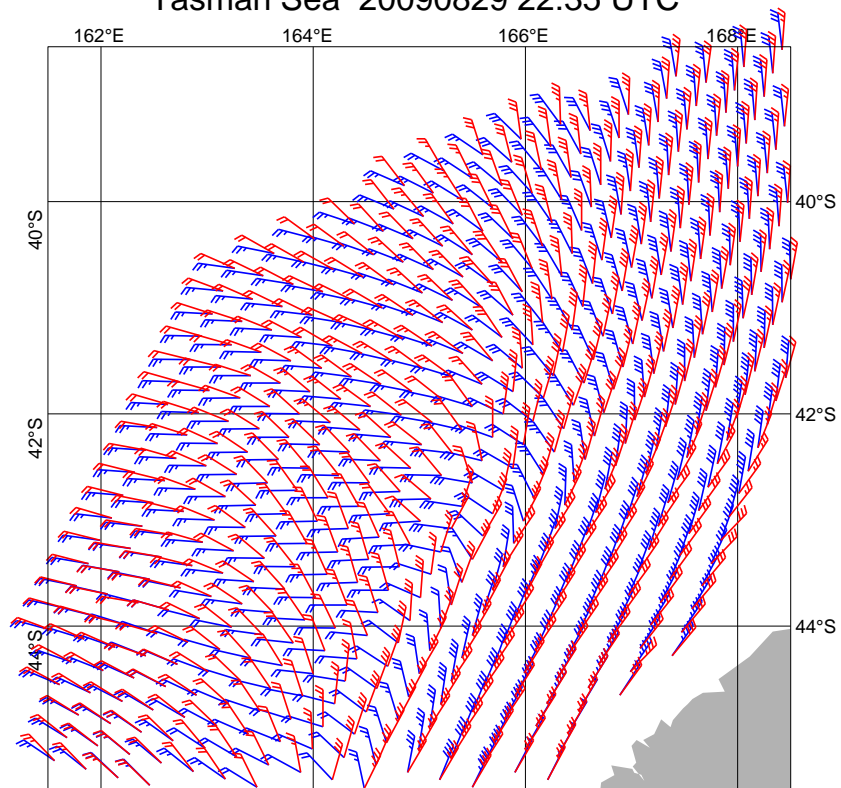


Figure 12

ECMWF 3-hourly First-Guess winds versus UWI winds
 from 2009082500 to 2009092818
 = 888521, db contour levels, 5 db step, 1st level at 4.5 db
 $m(y-x) = -1.01$ $sd(y-x) = 1.40$ $sdx = 3.50$ $sd_y = 3.22$ $pcxy = 0.957$

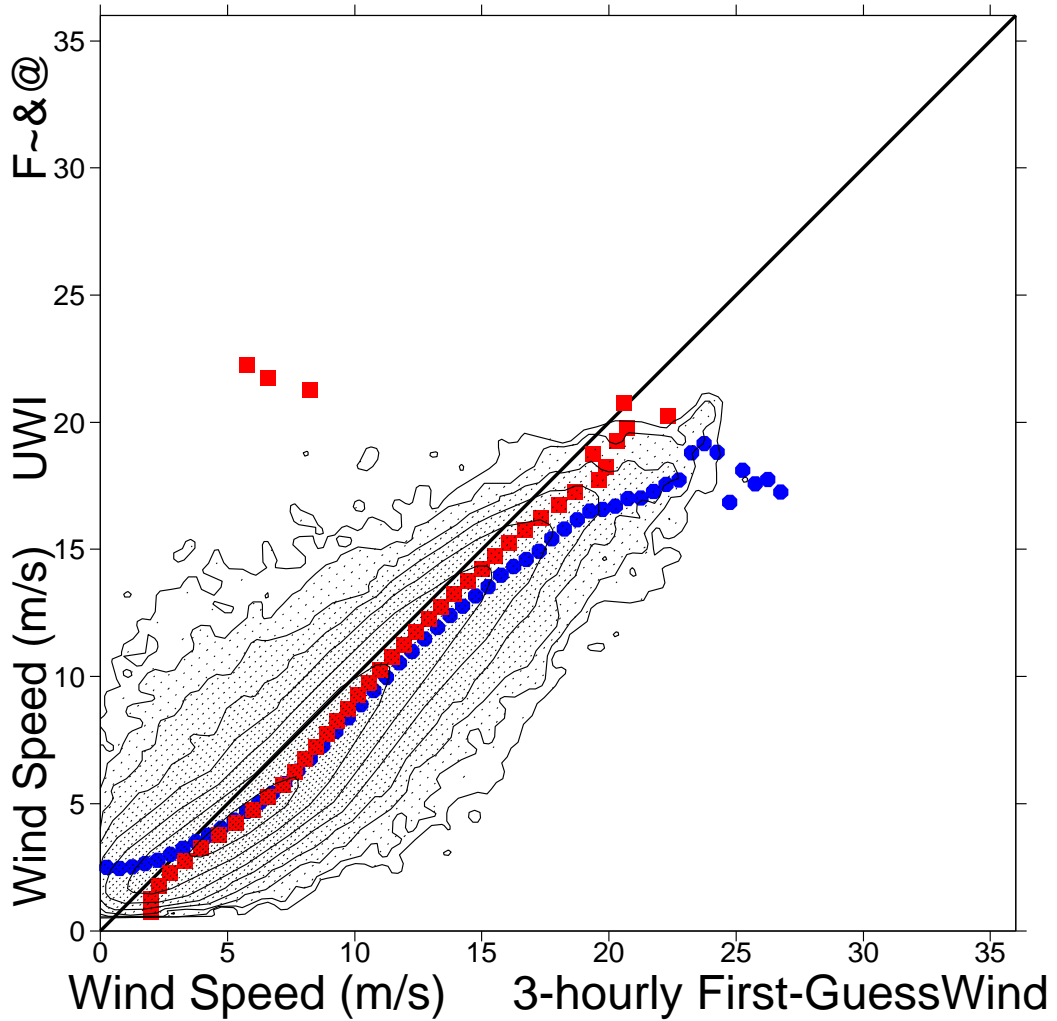


Figure 13

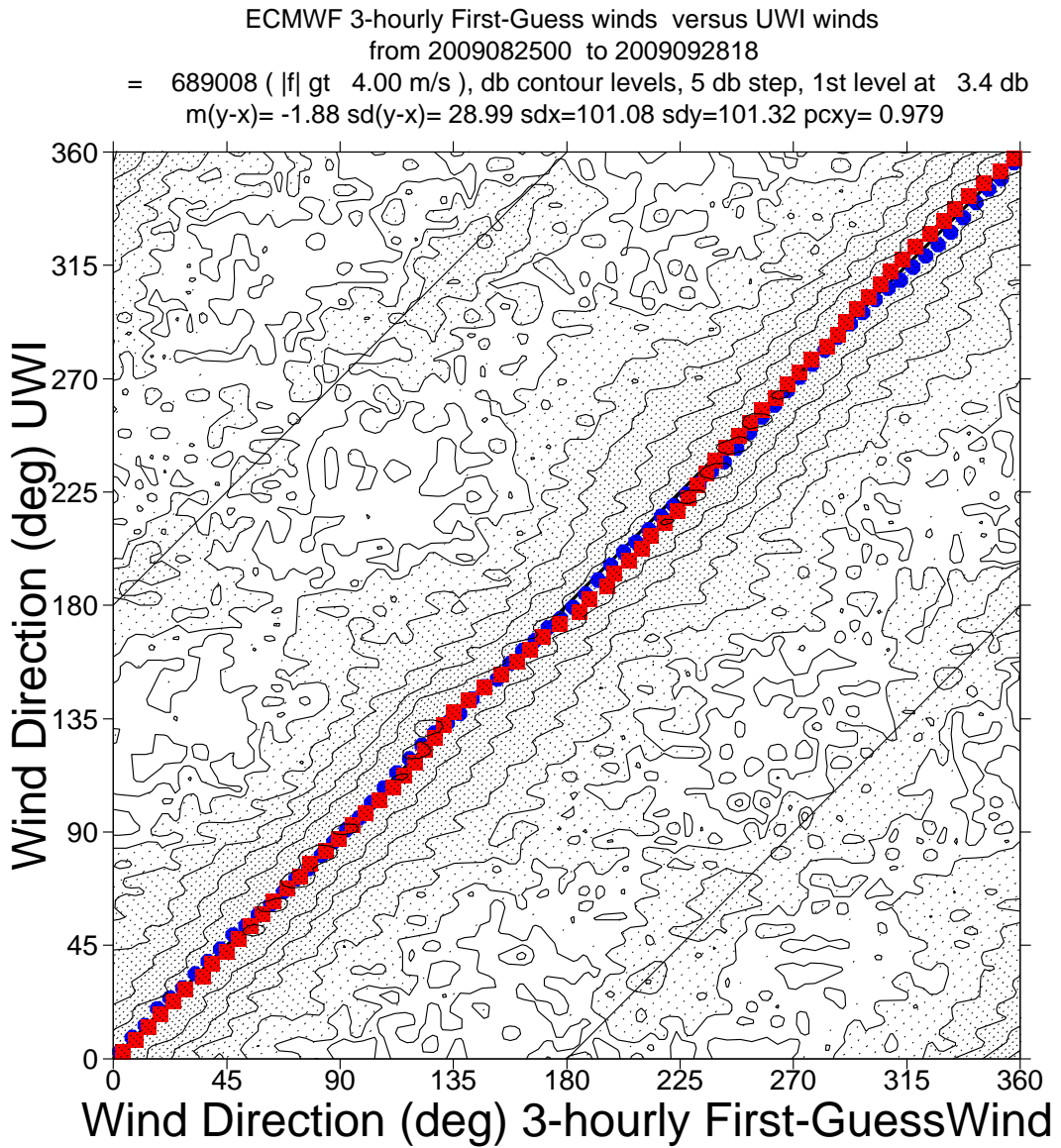


Figure 14

ECMWF 3-hourly First-Guess winds versus CMOD4 winds
from 2009082500 to 2009092818
= 879722, db contour levels, 5 db step, 1st level at 4.4 db
 $m(y-x) = -1.01$ $sd(y-x) = 1.40$ $sdx = 3.47$ $sd_y = 3.20$ $pcxy = 0.957$

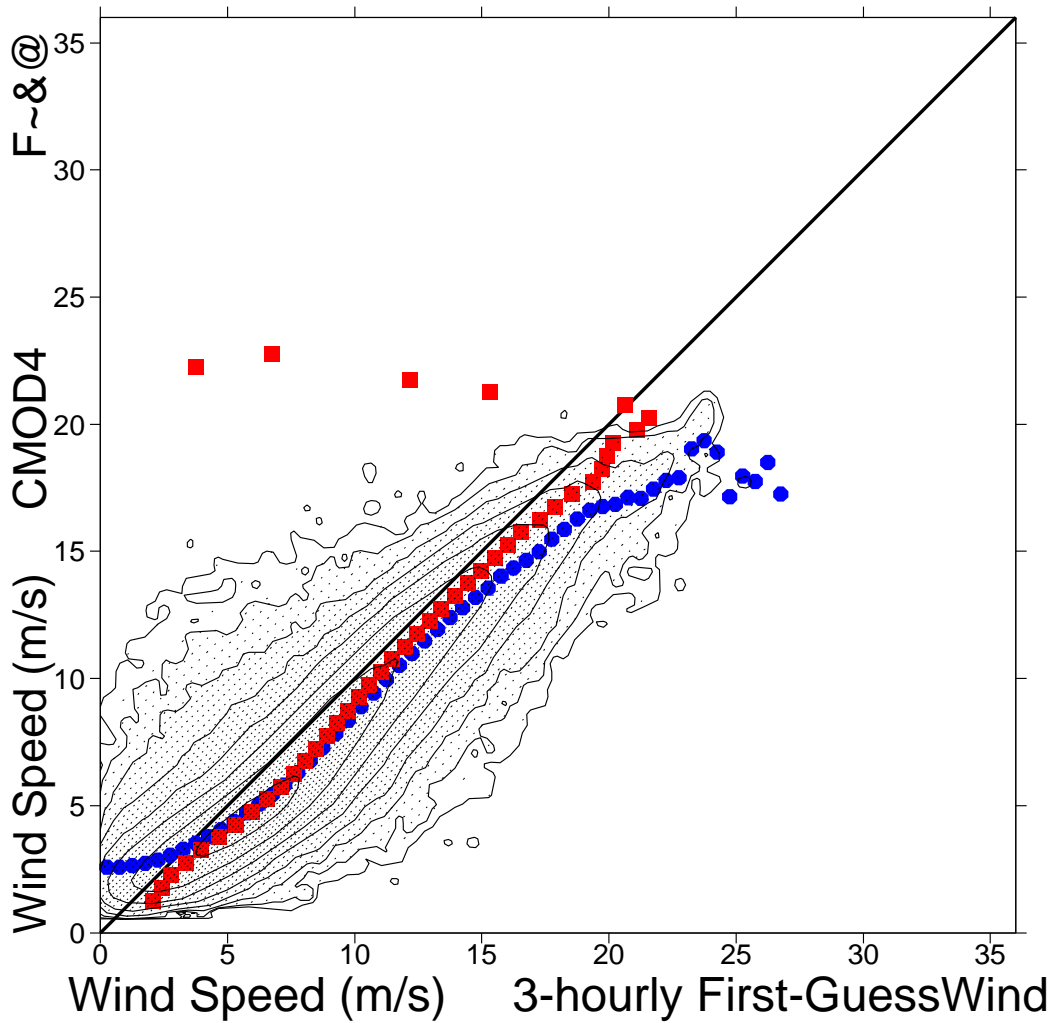


Figure 15

ECMWF 3-hourly First-Guess winds versus CMOD5 winds
from 2009082500 to 2009092818
= 862225, db contour levels, 5 db step, 1st level at 4.4 db
 $m(y-x) = -0.53$ $sd(y-x) = 1.35$ $sdx = 3.42$ $sdy = 3.31$ $pcxy = 0.959$

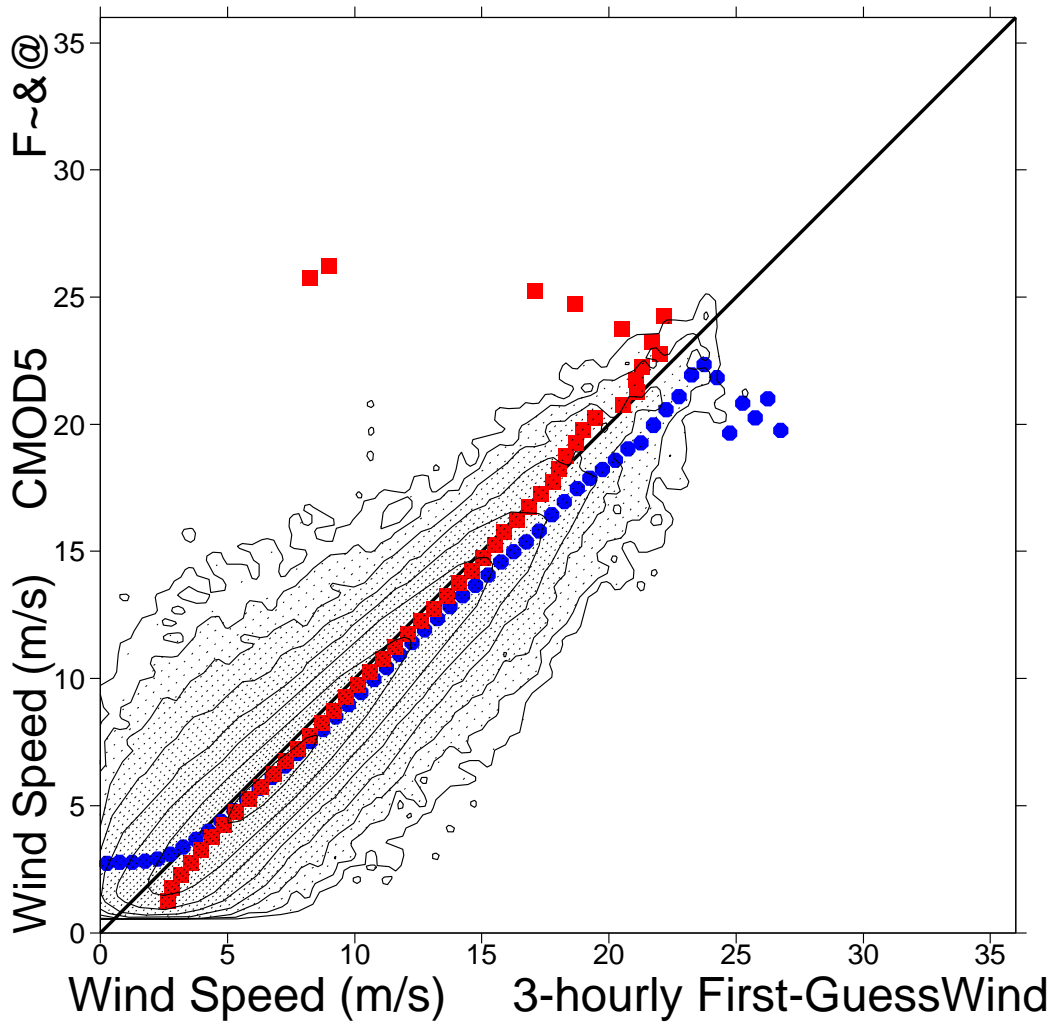


Figure 16

Figure 17

